NPAS1 Regulates Branching Morphogenesis in Embryonic Lung

Bernadette M. Levesque*, Shutang Zhou*, Lin Shan, Pamela Johnston, Yanping Kong, Simone Degan, and Mary E. Sunday

Department of Pediatrics, and Department of Pathology, Children's Hospital and Harvard Medical School, Boston, Massachusetts; and Department of Pathology, Duke University Medical Center, Durham, North Carolina

Drosophila trachealess (Trl), master regulator of tracheogenesis, has no known functional mammalian homolog. We hypothesized that genes similar to trachealess regulate lung development. Quantitative (Q)RT-PCR and immunostaining were used to determine spatial and temporal patterns of *npas1* gene expression in developing murine lung. Immunostaining for α-smooth muscle actin demonstrated myofibroblasts, and protein gene product (PGP)9.5 identified neuroendocrine cells. Branching morphogenesis of embryonic lung buds was analyzed in the presence of antisense or sense oligodeoxynucleotides (ODN). Microarray analyses were performed to screen for changes in gene expression in antisense-treated lungs. QRT-PCR was used to validate the altered expression of key genes identified on the microarrays. We demonstrate that *npas1* is expressed in murine embryonic lung. *npas1* mRNA peaks early at Embryonic Day (E)10.5–E11.5, then drops to low levels. Sequencing verifies the identity of *npas1* transcripts in embryonic lung. NPAS1 immunostaining occurs in nuclei of parabronchial mesenchymal cells, especially at the tracheal bifurcation. Arnt, the murine homolog of Tango (the heterodimerization partner for Trl) is also expressed in developing lung but at constant levels. *npas1*- or *arnt*-antisense ODN inhibit lung branching morphogenesis, with altered myofibroblast development and increased pulmonary neuroendocrine cells. On microarrays, we identify > 50 known genes down-regulated by *npas1*-antisense, including multiple genes regulating cell migration and cell differentiation. QRT-PCR confirms significantly decreased expression of the neurogenic genes RBP-Jk and Tle, and three genes involved in muscle development: β−ig-h3, claudin-11, and myocardin. Npas1 can regulate myofibroblast distribution, branching morphogenesis, and neuroendocrine cell differentiation in murine embryonic lung.

Keywords: branching morphogenesis; myofibroblasts; smooth muscle actin; cell migration; neuroendocrine cells

CLINICAL RELEVANCE

This research identifies NPAS1 as a novel transcription factor regulating branching morphogenesis in murine lung buds. NPAS1 antisense oligos inhibit branching via a mechanism involving arrested myofibroblast migration and neuroendocrine cell hyperplasia.

Lung morphogenesis is the result of complex interactions among multiple transcription factors, growth factors, and signaling pathways (1–4). Tracheal development in *Drosophila melanogaster* provides a simple model for investigating analogous genes involved in respiratory system development (5). Trachealess (*trl*) is the master regulatory gene because null mutation of *trl* leads to complete absence of the fly respiratory system (6). Trl also regulates downstream branching morphogenesis of the developing tracheal system (6, 7). Trl is a transcription factor (TF) with a basic helix-loop-helix (bHLH) domain and two "PAS" domains (6). Several other PAS domain genes have been cloned, including periodicity (*per*), *single-minded* (*sim*), and *aryl hydrocarbon nuclear translocator* (*arnt*), all of which collectively led to the designation of this family of TFs as "PAS" (per-arnt-sim) domain proteins. We became particularly interested in *npas1* because this gene is closely homologous to Drosophila *trl*. Amino acid alignment scores to the Drosophila Trl amino acid sequence on a pam250 matrix are for 393 for mouse Npas1, versus 335 for mouse Sim2 versus 210 for Arnt. We are interested in Arnt because Tango, its fly homolog, is required for Trl function via formation of heterodimers (8, 9), leading to regulation of the migration of the first tracheoblasts. This signaling initiates a developmental cascade critical for Drosophila tracheogenesis (9). *Breathless* (Drosophila fibroblast growth factor [FGF] receptor [FGFR]), *branchless* (Drosophila FGF), and *sprouty*, an FGF signaling antagonist, function downstream from Trl and also regulate tracheal branching (9). *Notch*, *delta*, and *enhancer of split* mutants have pleiotropic effects, including tracheal defects and increased neurogenesis (9). Similarly, pleiotropic signaling mechanisms with a role in both lung and tracheal development include FGF10 (2), the Nkx2.1 (1), and Notch-1 (10).

Functional information is now available for several PAS proteins. Murine NPAS1 (11, 12) is a PAS protein expressed in the central nervous system (CNS), where it regulates complex behaviors (13–15). In previous studies in other laboratories, *npas1* mRNA was not detected in either adult murine lung or whole embryos before Embryonic Day (E)13 using Northern blot analyses (12). Npas1-null mice did not have any apparent pulmonary phenotype, suggesting that either it has no role in lung development, or that the phenotype may occur only in certain genetic backgrounds, or that there is functional redundancy with other genes. However, there has been no known direct analysis of lung histopathology in *npas1*-null mice, nor any functional assay related to lung development in these mice. It is known that *in vitro* functional assays can be more sensitive than phenotypic analysis of knockout mice because short-term gene knock-down does not allow sufficient time for compensatory gene upregulation that can occur in knockout mice (16, 17). Similarly, in reports of *npas2* and *npas3*-null mice, there has been no report of pulmonary abnormalities. Consistent with *arnt* being ubiquitously expressed, *arnt*-null mice are embryonic

(*Received in original form August 24, 2006 and in final form October 2, 2006*)

* These authors contributed equally to this paper.

This work was supported by NIH grant #2RO1 HL44984 (M.E.S.) and NRSA training grant (B.M.L.).

Correspondence and requests for reprints should be addressed to Mary E. Sunday, M.D., Ph.D., Department of Pathology, Duke University Medical Center, Research Drive, Carl Building, Room 0043, Durham, NC 27710. E-mail: mary.sunday@duke.edu

This article has an online supplement, which is accessible from this issue's table of contents at www.atsjournals.org

Am J Respir Cell Mol Biol Vol 36. pp 427–434, 2007
Originally Published in Press as DOI: 10.1165/rcmb.2006-0314OC on November 16, 2006
Internet address: www.atsjournals.org

lethal before E14, but the hemizygous arnt-null mice do not have any obvious defects. Hypoxia-inducible factor (HIF)-1α and HIF-2α are additional PAS domain genes known to be of functional significance in lung vascular development (18, 19), but these are expressed in later fetal lung development (≥ E15.5) when alveolar capillary development begins.

None of the potential TRL homologs has been previously demonstrated *in vivo* to be associated with a mammalian respiratory phenotype. In the present study, we use a sensitive *in vitro* functional assay to test the hypothesis that NPAS1 can regulate lung development.

This work was presented in part at the International Conferences of the American Thoracic Society in 2003 and 2004 (20, 21).

MATERIALS AND METHODS

RNA Analyses

Total RNA was isolated from developing lungs from timed-pregnant Swiss-Webster mice (Taconic Laboratories, Germantown, NY) using TRIzol reagent (Invitrogen, Carlsbad, CA). cDNA was synthesized with SuperScript-III First-strand Synthesis System (Invitrogen). For QRT-PCR, primer pairs were designed to span introns (*see* online supplement for primer sequences) using Primer Express-3.0 (Applied Biosystems, Foster City, CA). For real-time-PCR, cDNA from 200 ng RNA, 0.5 μM primer pair, and 0.5 μM probe (Integrated DNA Technologies, Coralville, IA) were combined in Taqman Universal PCR Master-Mix (Applied Biosystems) and run in ABI-PRISM 7,300 (Applied Biosystems) at 50°C for 2-min, 95°C for 10 min, then 45-cycles at 95°C for 15 s each and 60°C for 1 min. Sequences of primers and probes for QRT-PCR of *npas1*, *sim2*, *arnt*, and β-*actin* are given in Table E1 in the online supplement. Sequences of primers and probes for QRT-PCR of *claudin 11*, *myocardin*, β-*ig-H*, *RBPsuh, Tle, npas1* and β-*actin* are given in Table E2.

Antisense Oligodeoxynucleotide Treatment of Developing Lungs

E11.5 embryonic lungs were cultured on Transwell inserts as described (10). Specific oligodeoxynucleotides (ODN) (primer sequences given in online supplement) were added to the media, changed daily. Cultures were incubated for 2–6 d. Lungs were photographed at 0 and 48 h.

Immunohistochemistry

Lungs were fixed in 4% paraformaldehyde and embedded in paraffin. Immunostaining for proliferating cell nuclear antigen (PCNA), smooth muscle actin (SMA), and protein gene product (PGP)9.5 was performed using the ABC method (Vector Laboratories, Burlingame, CA) as described (10). Anti-NPAS1 antibody (ProSci, Inc., Poway, CA) was used at 1:100. Anti-SMA murine monoclonal antibody (Dako Laboratories, Carpinteria, CA) was used at 1:125; anti-PGP9.5 rabbit polyclonal antibody (Ultraclone, Isle of Wight, UK) was used at 1:1,000. Slides were counterstained with methyl green.

RNA Microarray Analyses

Total RNA was prepared from five separate experiments in which E11.5 lung buds were treated with *npas1*-AS or -sense for 48 h. cDNAs were prepared and microarrays were hybridized and analyzed as detailed in the website for the Harvard Partners Center for Genomics and Genetics at http://www.hpcgg.org/News/MicroarrayDocument.pdf.

The bio-informatics pipeline for microarray data analysis and reporting was accomplished through integration with an analysis/workflow tool called GenePattern (http://www.broad.mit.edu/cancer/software/genepattern/). Normalized data for each array were exported to the Partners HPCGG Bioinformatics Server (http://portal.hpcgg.org), merged with updated gene annotation data for each probe set on the array, and downloaded for further data visualization and analysis.

RESULTS

QRT-PCR for NPAS1, Arnt, and Sim2

To determine temporal patterns and relative levels of gene expression, real-time quantitative RT-PCR (QRT-PCR) was performed for *npas1* and *arnt* using mRNA from murine lung from E10–E18 and postnatal day 1 (P1) (Figure 1a). Transcript levels were normalized for β-*actin* and expressed relative to the unit level defined in E11.5 lung buds. Although *arnt* mRNA levels change minimally during development (Figure 1a), *npas1* is expressed in embryonic lung during a specific developmental window. The level of *npas1* mRNA is highest at E10.5–E11.5, then markedly declines at E12.5 (Figure 1a and data not shown). As a specificity control, we also performed QRT-PCR for sim2, because sim2-null mice have normal lung development (22). Sim2 is expressed at high levels from E10.5–E16.5, when mRNA levels drop markedly.

NPAS1 Immunostaining

We then performed immunohistochemistry to localize NPAS1 protein in paraffin sections of embryonic lung (Figures 1b–1c). E11.5 lung buds were cultured for 48 h with *npas1* sense ODN. NPAS1 immunostaining is present in parabronchial mesenchymal cells and a few epithelial cells in the region of branchpoints (Figure 1b, *large arrows*). At higher magnification, NPAS1 is visualized in nuclei as strong, punctate immunostaining of nucleoli predominantly in mesenchymal cells immediately adjacent to branchpoints (Figure 1c, indicated by *long thin arrows*). NPAS1 immunostaining of another E11.5 lung bud from the same litter treated with *npas1*-AS ODN demonstrates abrogation of NPAS1 immunostaining in the parabronchial mesenchyme and the epithelium at the branchpoint (Figure 1d). A lower level of NPAS1 immunostaining remained in the bronchial ganglia (*arrow*), which is likely to represent relatively higher intracellular levels of NPAS1 in neurons, similar to neuropeptide levels observed using limiting dilution immunoperoxidase analysis (23). As an additional control, a section of the same *npas1* sense-treated lung bud shown in Figures 1b and 1c was stained using polyclonal rabbit IgG at the same protein concentration as the affinity-purified rabbit anti-NPAS1. As shown in Figure 1e, this section is devoid of any immunostaining.

We also performed immunostaining for NPAS1 at two later time points during fetal lung development. At E15.5, NPAS1 is strongly detected in nuclei of numerous mesenchymal cells, especially in the vicinity of branchpoints, in the cytoplasm of epithelial cells lining large airways (Figure 1f), and in nerve fibers and ganglia (data not shown). Lower levels of NPAS1 immunostaining are detected in cytoplasm of epithelial cells lining primitive alveoli and in nuclei of less than half of the airway epithelial cells. At E18.5, the only strong NPAS1 immunostaining is present in nerve fibers and ganglia, with weak to moderate staining of nuclei of epithelial cells lining the developing fetal airways (Figure 1g). These temporal and spatial patterns of NPAS1 antigen expression are consistent with a major role for this protein as a regulator of epithelial–mesenchymal interactions during early lung embryogenesis.

NPAS1 and Branching Morphogenesis

We then evaluated whether *npas1* or *arnt* gene expression in embryonic lung might play a functional role in morphogenesis. E11.5 lungs from timed pregnant Swiss-Webster mice were placed in culture with either sense or AS ODN in BGJb media. At this time point, the lung consists of the trachea, primary bronchi, and lung buds corresponding to the five future lobes of the murine lung. The number of lung buds at time zero (E11.5) ranged from five to nine. Littermates were used for all comparisons of sense and AS ODN. Lung buds were photographed at time zero and 48 h later for counting peripheral buds. The percent change from 0 to 48 h was calculated and compared with lungs from littermates treated with the corresponding sense ODN or with media alone. Dose–response studies were performed for

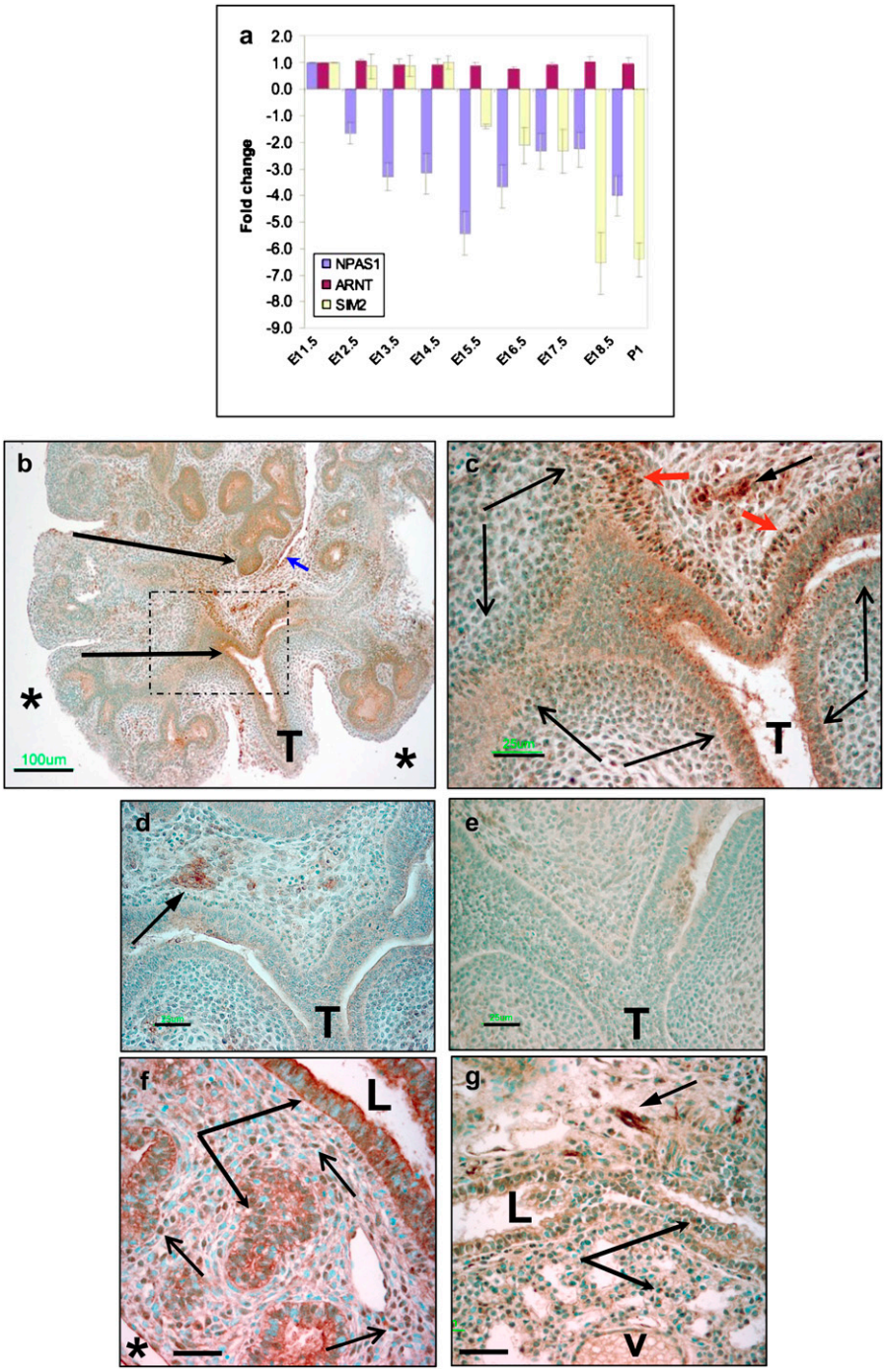

Figure 1. Ontogeny of NPAS1 mRNA and protein expression in murine lung. (*a*) Real-time QRT-PCR was used to quantify *npas1* mRNA levels in fetal lung, normalized to β-*actin* levels in the same RT reactions, and compared with levels at E11.5, which was defined as a unit level of one. For comparison, *arnt* and *sim2* mRNA levels were also quantified. Whereas *arnt* mRNA levels are essentially unchanged from E11.5 to P1, *npas1* drops at E12.5, and *sim2* drops at E16.5. (*b–e*) Immunoperoxidase staining of E11.5 lung buds with rabbit polyclonal anti-NPAS1 antibodies (*b–d*, *e–f*) or normal rabbit IgG control antibodies. Lung buds were cultured for 48 h with *npas1*-sense ODN (*b*, *c*, *e*) or with *npas1* AS ODN (*d*). *Bar in lower left hand corner* in *b* = 100 μm, and in *c–e* = 25 μm. T, trachea; * pleural surface, *long arrows* indicate NPAS1+ epithelial cells, and *short arrow* indicates NPAS1+ mesothelial cells. *Dotted lines* in *b* demarcate region that is enlarged in *c*. In *c*, *short red arrowheads* indicate strongly NPAS1+ nuclei of parabronchial myofibroblasts just inferior to the tracheal bifurcation. *Short black arrow* with *solid arrowhead* in *upper right hand corner* indicates NPAS1+ neurons and nerve fibers. *Long thin arrows* flank stretches of NPAS+ myofibroblasts arching along branchopoint, demonstrating apparent nucleolar immunostaining. (*f–g*) Immunoperoxidase staining of lung tissue from E15.5 (*f*) and E18.5 (*g*) embryos with rabbit polyclonal anti-NPAS1 antibodies. (*f*) At E15.5, there is strongly positive cytoplasmic staining of epithelial cells (*long arrows* with *solid arrowheads*), especially for epithelium of larger airways (L = airway lumen), with moderately positive NPAS1 immunostaining of most distal epithelial cells. There is also strong NPAS1+ immunostaining of many nuclei of mesenchymal cells (representative nuclei indicated by *short thin arrows*). *Bar* in *lower left hand corner* = 25 μm; * pleural surface. (*g*) At E18.5, the only intense npas1 immunostaining is present in nerve fibers and ganglia (*short arrow* with *solid arrowhead*, *upper right hand corner*). NPAS1+ nuclei occur only infrequently in the epithelium (indicated by two *long arrows*) of airways (L = airway lumen) and primitive alveoli (*lower arrow*). *Bar* in *lower left hand corner* = 25 μm; v, blood vessel.

npas1 and *arnt* at 0.5–10 μM final. The greatest effect on lung bud phenotype (*see below*) was observed at 5–10 μM, so we used 5 μM for all subsequent experiments. QRT-PCR was used to validate reduction of these mRNAs by 5 μM of the AS ODN in E11.5 lung bud cultures (three experiments, three to four lung buds pooled per experiment from each of two litters) compared with the sense controls. Compared with *npas1*-sense–treated cultures, *npas1*-AS reduced *npas1* mRNA levels by 48.0 ± 0.4% ($P < 0.0001$). Compared with *arnt*-sense–treated cultures, *arnt*-AS reduced arnt mRNA levels by 15 ± 2% ($P < 0.0001$). Similarly, *sim2*-AS reduced *sim2* mRNA levels by 24 ± 3% ($P < 0.0001$). Finally, mRNA levels for *arnt* and *sim2* were not significantly altered by *npas1*-antisense compared with *npas1*-sense (reduced by 4% and 9%, respectively).

To verify that the ODN were taken up by potential target cells in the lung buds, we added Alex-488–labeled *npas1*-antisense or -sense ODN to the cultures. After 24 h of incubation, both AS (Figures 2a and 2b) and sense (Figures 2c and 2d) ODN were concentrated predominantly in the mesenchyme (Figures 2b and 2d).

We then used unlabeled ODN for the functional studies. After 48 h, there is no effect of *npas1*-sense or *arnt*-sense ODN on branching morphogenesis (Figures 2e and 2g) compared with untreated control lung buds from the same litter (data not shown), whereas *npas1*-AS and *arnt*-AS ODN (Figures 2f and 2h) significantly inhibit branching morphogenesis compared with the corresponding sense controls. Compared with the corresponding sense controls, branching morphogenesis of E11.5 lung

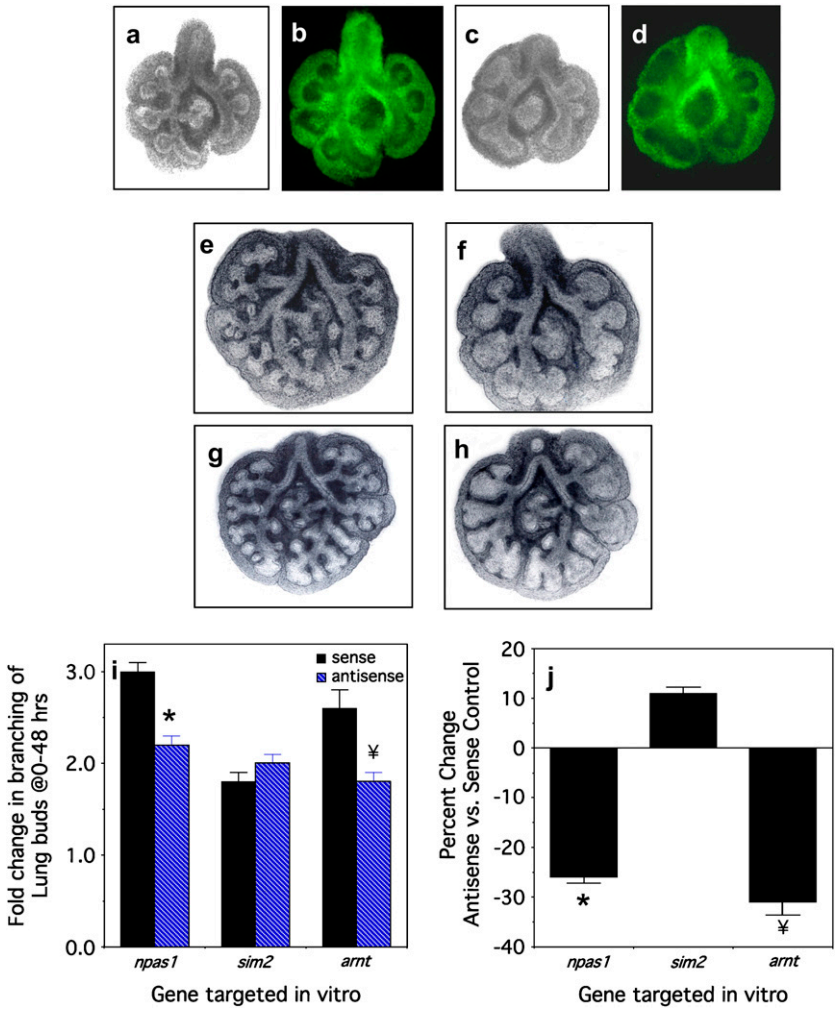

Figure 2. Branching morphogenesis of murine lung buds is diminished by *npas1* or *arnt* antisense treatment. (*a*, *b*) A representative E11.5 lung bud (*a*, phase contrast; *b*, fluorescence miscroscopy) treated with fluoresceinated *npas1*-sense ODN at 5 μM for 24 h demonstrates widespread uptake of the ODN by mesenchymal tissue regions, especially adjacent to the epithelium in the vicinity of branchpoints. (*c*, *d*) Similarly, a representative E11.5 lung bud (*c*, phase contrast; *d*, fluorescence microscopy) treated with fluoresceinated *npas1* AS ODN at 5 μM for 24 h demonstrates widespread uptake of the ODN by mesenchymal tissue regions, especially adjacent to the epithelium in the vicinity of branchpoints. (*e*) Treatment with *npas1*-sense at 5 μM for 48 h has no effect on branching morphogenesis of E11.5 lung buds. (*f*) Treatment of a lung bud from the same litter as in *a* with *npas1* AS leads to decreased numbers of peripheral buds, which are dilated and dysmorphic, ending in rounded sacs. (*g*) Treatment with *arnt*-sense at 5 μM for 48 h has no effect on branching morphogenesis. (*h*) Treatment of lung buds from the same litter as in *c* with *arnt*-AS results in decreased numbers of peripheral buds, which are dilated and misshapen, ending in rounded and box-like sacs. (*i*) The pooled results of the branching assay are given as the percent change in peripheral buds from 0–48 h, with the following numbers of lung buds (3–4 per litter treated with a given ODN: *npas1*-sense [$n = 26$] versus *npas1* AS [$n = 28$], * $P < 0.0001$; *arnt*-sense [$n = 13$] versus *arnt* AS [$n = 15$], ¥ $P < 0.003$; and a specificity control, *sim2*-sense [$n = 25$] versus *sim2* AS [$n = 27$], $P = 0.12$). (*j*) The same data as in (*e*) is given here as the percent change in branching observed with the AS ODN as compared with the corresponding sense control.

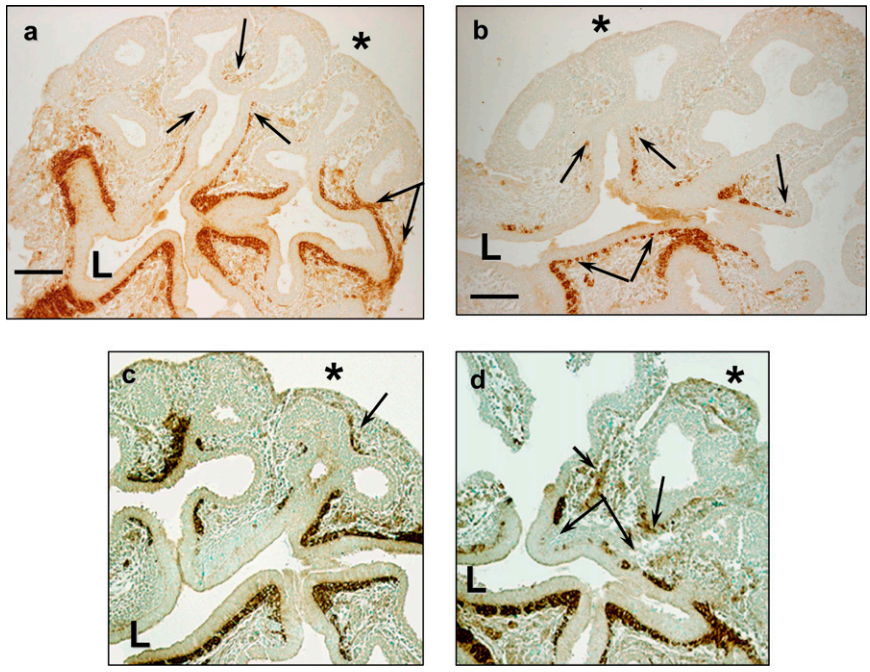

Figure 3. Immunostaining for SMA in E11.5 lungs treated with *npas1*- or *arnt*-antisense. (*a*) Lungs cultured with *npas1* sense ODN have near-continuous SMA staining from the tracheal bifurcation (below "L"), along the conducting airways out to the primitive alveolar buds (as indicated by *double arrows*). *Single arrows* indicate the most distal SMA cells. L, proximal airway lumen; * pleural surface; *bar* in *lower left hand corner* = 50 μm. (*b*) Lungs cultured with *npas1* AS have discontinuous and/or arrested myofibroblast development occurring about halfway down the developing airway (*single arrows*). Discontinuous SMA+ immunostaining is indicated by *joined double arrows*; L, proximal airway lumen; * pleural surface; *bar* in *lower left hand corner* = 50 μm. (*c*) Lungs cultured with *arnt*-sense also have continuous SMA staining along most of the conducting airways (L, proximal airway lumen) out to near the pleural surface (*arrow* indicates SMA+ cells near pleural surface, indicated by *asterisk*). (*d*) Lungs cultured with *arnt* AS have discontinuous and/or arrested myofibroblast development along developing airways (*arrows*). Pleural surface is indicated by an *asterisk*. Discontinuous SMA+ immunostaining is indicated by *double arrows*; some SMA+ cells are not clearly associated with airways (*small arrowhead*). L, proximal airway lumen; * pleural surface; *bar* in *lower left hand corner* = 50 μm.

buds is decreased by 26% by *npas1*-AS (Figures 2f and 2i), and also reduced 32% by *arnt*-AS (Figures 2h and 2i). There is no significant difference in branching morphogenesis between lung buds treated with *npas1*-sense or *arnt*-sense and media-alone controls from the same litter (data not shown), in contrast to the abnormal morphology of lungs cultured with *npas1*- or *arnt*-antisense ODN (Figures 2f and 2h). These data are consistent with heterodimer formation by NPAS1 and Arnt to form a functional complex to regulate transcription, analogous to TRL and Tango in Drosophila (24). Thus, the effect of *arnt*-AS may be due to decreased NPAS1 function because Arnt is a ubiquitous dimerization partner for many PAS proteins (8, 9). S*im2*-antisense did not alter branching morphogenesis compared with the *sim2*-sense control, whereas *sim2*-sense alone decreased branching by 29 ± 2% compared with media alone ($P = 0.0003$). However, *sim2*-AS did decrease *sim2* mRNA levels by 24% compared with *sim2*-sense, indicating that *sim2*-AS does have a specific effect on *sim2* mRNA levels, in spite of which there is no effect on branching morphogenesis. Thus, effects of antisense ODN are most valid when antisense groups are compared with the corresponding sense control to correct for nonspecific effects of the ODN (25).

We used classical histopathologic methods to compare effects of *npas1*-AS and *arnt*-AS on cell proliferation, including both BrdU incorporation and immunostaining for PCNA. Extensive analyses of all sections from multiple experiments demonstrate that cell proliferation is not appreciably altered in *npas1*- or *arnt*-AS–treated lungs compared with sense controls (data not shown). Similarly, there is no visible change in apoptosis by *npas1*-antisense treatment according to either *in situ* TUNEL analysis with the ApopTag kit or histologic detection of TUNEL-positive apoptotic bodies (data not shown).

Myofibroblasts in NPAS1-AS–Treated Lung Buds

We next used immunohistochemistry to explore cell differentiation in *npas1*- and *arnt*-AS–treated lung buds. SMA immunostaining demonstrates a consistently altered distribution of myofibroblasts in E11.5 lung buds cultured with either AS for 2 d. Compared with sense-treated lung buds from littermates (Figures 3a and 3c), we observed reduced extension of myofibroblasts within the subepithelial mesenchyme along the branching epithelial tubes (Figures 3b and 3d). The myofibroblasts in lung buds treated with *npas1*-AS (Figure 3b) or *arnt*-AS (Figure 3d) appear as irregular clusters or clumps of cells that are discontinuous and rounded up, extending only about halfway down the primitive bronchial tree (Figure 3d, *arrows*). In contrast, in sense-treated lungs (Figure 3c, *arrows*) or lungs cultured without any ODN (data not shown) the myofibroblasts extend evenly and taper off continuously from the proximal airways down to the peripheral buds.

Neuroendocrine Cells in NPAS1-AS–Treated Lung Buds

Considering our earlier observations of altered lung branching morphogenesis together with increased numbers of neuroendocrine (NE) cells when Notch signaling is inhibited, we analyzed the expression of an NE cell marker in *npas1*-AS–treated lung buds (10). We also chose to study NE cells because they are known to be the first epithelial cell to differentiate in ontogeny and can be detected after about one week of culture of E11.5 lung buds (26). After 6 d in culture, occasional NE cells can be visualized in *npas1*-sense–treated controls by immunostaining for the early neural/NE cytoplasmic marker PGP9.5 (Figures 4a and 4b). Other NE markers such as calcitonin gene-related peptide are not yet detectable (data not shown). These NE cells are distributed both proximally and distally in the primitive lung buds, extending from the mainstem bronchi down at least three airway generations. Lung buds treated with media alone without ODN for 6 d also had infrequent NE cells (data not shown). In contrast, lung buds treated with *npas1*-AS for 6 d (Figures 4c and 4d) have markedly increased numbers of NE cells, occurring both as single cells (*thin arrows*) and as clusters within the primitive airway epithelium (*thick arrows*). Occasionally linear arrays of NE cells are seen (*double arrow* in Figure 4c). In *npas1*-AS–treated lung buds, the NE cells are distributed both proximally and distally, beginning in the mainstem bronchi, and throughout the epithelium for at least three airway generations. Quantification of relative numbers of NE cells in these lung buds normalized for the tissue area of each lung bud is shown in Figure 4e. In lung buds treated for 6 d with *npas1*-AS ODN, there is a highly significant increase in both the number of PGP+ foci (5.6-fold increased) and the total number of NE cells (9-fold increased) per in^2 area of lung bud tissue ($P < 0.0001$). There is also a significant increase in the number of NE cells per focus (1.7-fold increased, $P < 0.012$).

mRNA Microarray Analyses

To begin to investigate molecular mechanisms underlying the observed morphologic changes, we performed expression profiling of lung buds treated with *npas1*-AS versus -sense controls from the same litters. RNA was extracted from pooled lung samples from five separate experiments (three to six lung buds per experiment) after 48 h of culture. Microarray analysis was performed by probing five pairs of Affymetrix 430A-2.0 gene array chips (Affymetrix, Union City, CA) using cDNA prepared from *npas1*-AS– versus *npas1*-sense–treated lung buds. Detailed protocols are given elsewhere (27).

The cumulative data were analyzed by excluding all samples with an absent signal in either AS- or sense-treated mRNA samples. The remaining genes were sorted and selected for $P < 0.05$ and fold-change > 3-fold. We identified a total of 157 genes consistently down-regulated and 11 genes consistently up-regulated in all five experiments (listed in Table E3). Of these genes, 9 are duplicates and 62 are unidentified genes (24 RIKENs, 20 unknowns, 1 open reading frame, and 17 ESTs). Excluding these genes results in 93 genes down-regulated by 1/3 or less by *npas1*-AS and 5 genes up-regulated by 3-fold or more by *npas1*-AS. None of the up-regulated genes appear to be of functional significance. At least 13 of the genes down-regulated by *npas1*-AS have known functions in regulating cell shape, cell adhesion, cell migration, extracellular matrix formation, and/or smooth muscle cell differentiation (Table 1). At least 4 of these genes plus 12 additional genes are known to play a role in normal development and/or angiogenesis, including 5 transcription factors (Table 1) (also listed in Tables E3 and E4). Other down-regulated genes are components of signal transduction cascades, many of which are involved in G-protein signaling, which can regulate cell migration. Finally, some of the genes down-regulated by *npas1*-AS are likely to play a role in lung development, including sonic hedgehog (Shh) signaling molecules (hhip, Hoxb4, Tbx5, dachshund, IGF-I).

Some genes down-regulated by *npas1*-AS are known regulators of CNS development, including two neurogenic genes (RBPsuh, suppressor-of-hairless, and Tle, transducin-like enhancer-of-split), which function in Notch-related lateral inhibition of neural/NE differentiation (28). This gene family also plays a major downstream role in tracheal development in Drosophila (9). Decreased expression of neurogenic genes would

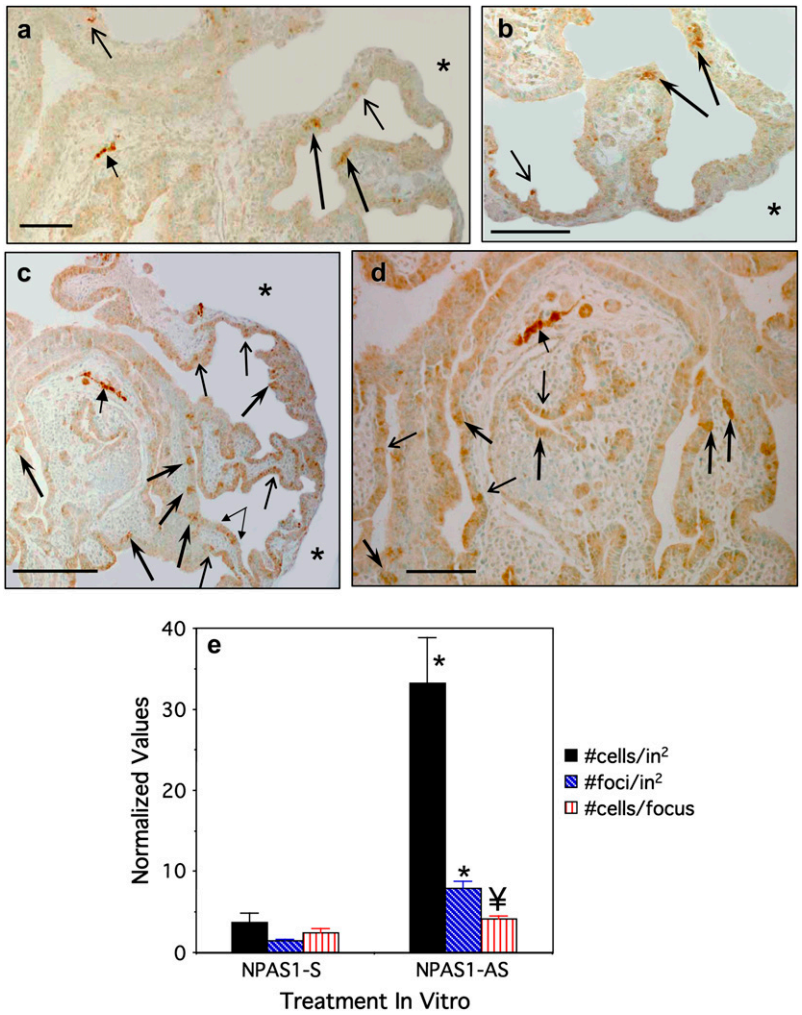

Figure 4. PGP9.5 Immunostaining in E11.5 lungs treated with *npas1*- or *arnt*-antisense. (*a*, *b*) Immunostaining of lung buds cultured for 6 d with *npas1*-sense oligos have occasional clusters of PGP9.5-positive NE cells scattered throughout the airway epithelium (*long dark arrows*) and also a few isolated NE cells (*short thin arrows*). As an internal positive control, a PGP9.5-positive nerve fiber is visible in the *mid-left field* of *a* (*solid arrowhead*). *Bars* in *lower left hand corner* = 50 μm. * Pleural surface. (*c*, *d*) Lungs cultured with *npas1* AS for 6 d have a marked increase in PGP9.5-positive NE cell clusters (*solid arrows*), as well as a modest increase in isolated NE cells (*thin arrows*). *Small linked arrows* in *lower right hand corner* of *c* indicate a stretch of linear NE cell hyperplasia. The internal positive control is a PGP9.5-positive nerve fiber (*arrowhead, upper left hand corner* of *c*, in which *asterisk* indicates pleural surface). *Bars* in *lower left hand corner* = 100 μm (*c*) and 50 μm (*d*). (*e*) Morphometric analysis for relative numbers of PGP9.5+ NE cells in E11.5 lung buds treated with *npas1*-sense or -AS ODN in culture for 6 d. We determined the number of PGP+ cell foci (including both isolated cells and clusters of ⩾ 2 cells) and the total number of PGP+ cells, both of which were normalized for the area of lung tissue present using Scion Image 1.62 software (Scion Corp., Frederick, MD) and density slice analysis. The number of PGP+ cells per focus was also calculated. Data shown represent the mean values ± SE for complete cross-sections of $n = 9$ (sense-treated lung buds) and $n = 14$ (AS-treated lung buds), representing pooled data from four experiments including matched controls from the same litters. * $P < 0.0001$ compared with npas1 sense control; ¥ $P < 0.012$ compared with sense control.

provide a mechanistic basis for increased pulmonary NE cells in *npas1*-AS–treated lungs.

To validate expression levels of several genes that would likely contribute to the altered morphogenesis that we observed in the lung buds, we performed QRT-PCR. The results of three pooled experiments are given in Figure 5. *Npas1* mRNA is reduced ~ 50%, consistent with earlier experiments. Both *RBPsuh* and *Tle* are decreased ~ 20%, which seems modest but is statistically significant. Diminished expression of both of these genes could function synergistically, because they are known to act in the same signaling pathway, leading to the observed increase in NE cells after 6 d in culture. Furthermore, *notch-1* AS treatment has been demonstrated to induce phenotypic changes in chick retina with as little as 20% reduction in *notch-1* mRNA levels (29). Last, but not least, RBP and other neurogenic genes in the Notch signaling pathway also play a major role in the determination of smooth muscle differentiation (30, 31), consistent with pleiotropic effects of decreased RBPsuh contributing to both increased NE cells and decreased smooth muscle development in E11.5 lung buds.

Gene expression for TGF-β-induced 68 kD, also termed "β-IG-H3" are reduced ~ 30% ($P < 0.005$). BetaIG-H3 is likely to play a role in lung development, being expressed at high levels in distal lung during organogenesis (32). It is present in the extracellular matrix, cytoplasm, and nuclei of smooth muscle cells in human airways and pulmonary vasculature, especially in the septal tips of alveolar ducts and alveoli, suggesting that it may have a morphogenetic role (33).

Claudin-11, also significantly decreased by *npas1*-AS with $P < 0.005$, is a transmembrane tight-junction protein that is homologous to Drosophila Megatrachea, which plays an important role in regulating morphogenesis of the Drosophila tracheal system (34). Claudin-11 deficiency could also lead to the distal airspace dilatation that we observe in *npas1*-AS–treated lung buds. Claudin-3 is expressed in chick lung buds during development (35). Claudin-5 localizes to junctions between cardiomyocytes and its deficiency is associated with dilated cardiomyopathy (36), suggesting that decreased claudin-11 could be linked to the abnormal shape and lack of continuity between myofibroblasts along airways of *npas1*-AS–treated lung buds.

Finally, down-regulation of myocardin gene expression ($P < 0.01$) could be consistent with impaired development of smooth muscle along developing airways (37). Myocardin is a transcription factor that has been shown to be necessary and sufficient for smooth muscle cell differentiation (37, 38).

Conclusions

In summary, we have demonstrated that *npas1* and *arnt* are expressed and functional in murine embryonic lung: knocking down *npas1* or *arnt* mRNA levels in lung bud cultures inhibits lung branching and myofibroblast development, analogous to decreased cell migration in Trl-null Drosophila. Furthermore,

TABLE 1. GENES DOWN-REGULATED IN LUNG BUDS BY NPAS1-ANTISENSE

Cell migration/adhesion/muscle development
Actin, alpha 2, smooth muscle, aorta*
Actin, gamma 2, smooth muscle, enteric
Angiopoietin 2 (inhibits angiogenesis)*
Claudin 11
Elfin (PDZ and LIM domain 1)
Junction cell adhesion molecule 3
Protocadherin beta 9 (Pcdhb9)
RHAMM (receptor for hyaluronic acid)*
Myocardin
Rab-2 (GTPase)\rho GTPase-activating protein 6
Transforming growth factor-beta induced, 68 kD
Transgelin
Tropomyosin 2, beta*
Cell differentiation/morphogenesis
Transcription Factors
Forkhead box C1 (Foxc1)
Homeobox B4 (Hoxb4)
Recombining binding protein suppressor of hairless (Rbpsuh)
Transducin-like enhancer of split 1 homolog (Tle1)
T-box transcription factor (Tbx5)
Other regulatory molecules
Adenylate cyclase 3
Endothelial differentiation, G-protein–coupled receptor 2*
Faciogenital dysplasia homolog
Fibrosin
Hedgehog-interacting protein (hedgehog antagonist)
Inhibitor of kappaB kinase gamma
Syndecan 2

* Role in angiogenesis.

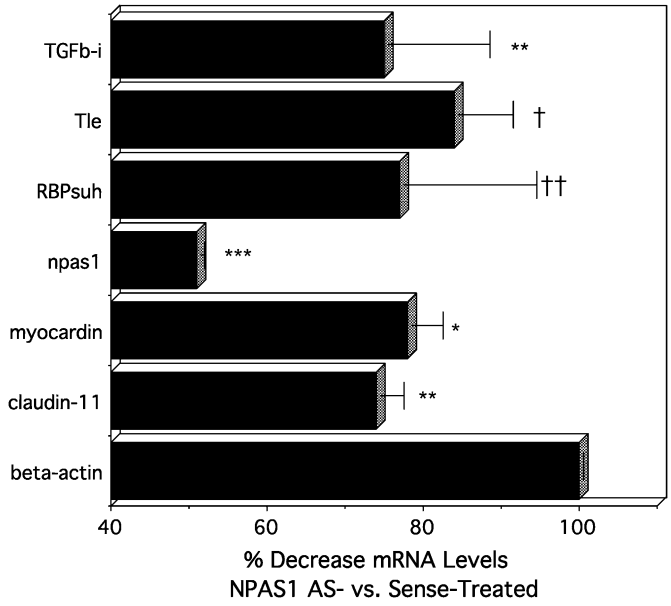

Figure 5. QRT-PCR validation of differential gene expression in E11.5 lung buds treated with NPAS1-antisense versus -sense ODN. The results given are the pooled data from three separate experiments using three independent RNA preparations from E11.5 lung buds treated with ODN for 48 h. Results are presented as mean percentage change ± SE, comparing *npas1*-AS–treated lungs versus *npas1*-sense–treated lungs. For comparison, β-actin is defined as 100% for *npas1*-AS relative to sense. Significance levels are: *** $P < 0.0001$; ** $P < 0.005$; * $P < 0.01$; †† < 0.02; † $P < 0.05$.

npas1-AS–treated lungs have down-regulated expression of numerous developmentally important genes. Two prominent clusters of inter-related genes that are down-regulated by *npas1*-AS are: first, genes controlling cell migration, adhesion, and/or smooth muscle development; and second, genes regulating neurogenesis. These observations provide a mechanistic basis for inhibition of branching and smooth muscle development and increased numbers of NE cells.

Myofibroblast migration is recognized to be a major factor in normal lung morphogenesis, especially during alveolarization (39). Similarly in Drosophila TRL functions by regulating cell migration during formation of the primary tracheal tube and also during branching morphogenesis (6, 9). Previously we demonstrated that *notch-1*-AS–treated lung buds have increased branching morphogenesis and increased numbers of NE cells (10). In Drosophila, Notch is implicated as a negative regulator of tracheal development downstream from TRL (9). The cumulative direct and circumstantial evidence suggests that *npas1* may be one functional mammalian homolog of the Drosophila *trl* gene. Despite high sequence conservation, in the CNS several other PAS proteins have been found to be biologically essential and functionally nonredundant (8). However, functional redundancy is common in developmental/biological processes that are essential for survival. We propose that functional redundancy of multiple signaling pathways activated by *npas1* could provide a selective advantage to preserve normal lung structure and function that are crucial for postnatal survival. Thus, our short-term *in vitro* studies are not incompatible with the apparent lack of a pulmonary phenotype in NPAS1 KO mice. In conclusion, the cumulative evidence indicates that NPAS1 can function as a proximal regulator of lung organogenesis, consistent with NPAS1 being a candidate mammalian homolog of TRL, the primary regulator of respiratory system development in Drosophila.

Conflict of Interest Statement: None of the authors has a financial relationship with a commercial entity that has an interest in the subject of this manuscript.

Acknowledgments: The authors thank Dr. Vance Morgan, Linette Mookanamparambil, and Deepti Anand in the Harvard Partners Center for Genetics and Genomics for carrying out the microarray analyses. The authors acknowledge the technical assistance of Fan Zhang.

References

1. Minoo P, Su G, Drum H, Bringas P, Kimura S. Defects in tracheoesophageal and lung morphogenesis in Nkx2.1(−/−) mouse embryos. *Dev Biol* 1999;209:60–71.
2. Lu J, Izvolsky KI, Qian J, Cardoso WV. Identification of FGF10 targets in the embryonic lung epithelium during bud morphogenesis. *J Biol Chem* 2005;280:4834–4841.
3. Weaver M, Batts L, Hogan BL. Tissue interactions pattern the mesenchyme of the embryonic mouse lung. *Dev Biol* 2003;258:169–184.
4. van Tuyl M, Post M. From fruitflies to mammals: mechanisms of signalling via the Sonic hedgehog pathway in lung development. *Respir Res* 2000;1:30–35.
5. Manning G, Krasnow MA. in Development of Drosophila melanogaster. Cold Spring Harbor Laboratory Press; 1993. pp. 609–685.
6. Wilk R, Weizman I, Shilo B-Z. *Trachealess* encodes a bHLH-PAS protein that is an inducer of tracheal cell fates in *Drosophila. Genes Dev* 1996;10:93–102.
7. Affolter M, Bellusci S, Itoh N, Shilo B, Thiery JP, Werb Z. Tube or not tube: remodeling epithelial tissues by branching morphogenesis. *Dev Cell* 2003;4:11–18.
8. Kewley RJ, Whitelaw ML, Chapman-Smith A. The mammalian basic helix-loop-helix/PAS family of transcriptional regulators. *Int J Biochem Cell Biol* 2004;36:189–204.
9. Metzger RJ, Krasnow MA. Genetic control of branching morphogenesis. *Science* 1999;284:1635–1639. (Review).
10. Kong Y, Glickman J, Subramaniam M, Shasafaei A, Allamneni KP, Aster JC, Sklar J, Sunday ME. Functional diversity of notch family genes in fetal lung development. *Am J Physiol Lung Cell Mol Physiol* 2004;286:L1075–L1083.

11. Brunskill EW, Witte DP, Shreiner AB, Potter SS. Characterization of npas3, a novel basic helix-loop-helix PAS gene expressed in the developing mouse nervous system. *Mech Dev* 1999;88:237–241.
12. Zhou YD, Barnard M, Tian H, Li X, Ring HZ, Francke U, Shelton J, Richardson J, Russell DW, McKnight SL. Molecular characterization of two mammalian bHLH-PAS domain proteins selectively expressed in the central nervous system. *Proc Natl Acad Sci USA* 1997;94:713–718.
13. Erbel-Sieler C, Dudley C, Zhou Y, Wu X, Estill SJ, Han T, Diaz-Arrastia R, Brunskill EW, Potter SS, McKnight SL. Behavioral and regulatory abnormalities in mice deficient in the NPAS1 and NPAS3 transcription factors. *Proc Natl Acad Sci USA* 2004;101:13648–13653.
14. Brunskill EW, Ehrman LA, Williams MT, Klanke J, Hammer D, Schaefer TL, Sah R, Dorn GW 2nd, Potter SS, Vorhees CV. Abnormal neurodevelopment, neurosignaling and behaviour in Npas3-deficient mice. *Eur J Neurosci* 2005;22:1265–1276.
15. Garcia JA, Zhang D, Estill SJ, Michnoff C, Rutter J, Reich M, Scott K, Diaz-Arrastia R, McKnight SL. Impaired cued and contextual memory in NPAS2-deficient mice. *Science* 2000;288:2226–2230.
16. Herradon G, Ezquerra L, Nguyen T, Silos-Santiago I, Deuel TF. Midkine regulates pleiotrophin organ-specific gene expression: evidence for transcriptional regulation and functional redundancy within the pleiotrophin/midkine developmental gene family. *Biochem Biophys Res Commun* 2005;333:714–721.
17. Iacobas DA, Urban M, Iacobas S, Spray DC. Transcriptomic characterization of four classes of cell-cell/cell-matrix genes in brains and hearts of wild type and connexin43 null mice. *Rom J Physiol* 2002–2003; 39–40:91–116.
18. Peng J, Zhang L, Drysdale L, Fong GH. The transcription factor EPAS-1/hypoxia-inducible factor 2alpha plays an important role in vascular remodeling. *Proc Natl Acad Sci USA* 2000;97:8386–8391.
19. Asikainen TM, Waleh NS, Schneider BK, Clyman RI, White CW. Enhancement of angiogenic effectors through hypoxia-inducible factor in preterm primate lung in vivo. *Am J Physiol Lung Cell Mol Physiol* 2006;291:L588–L595.
20. Shan L, Levesque B, Kong Y, Sunday ME. Genes encoding neuronal PAS domain proteins (NPAS1 & 3) and aryl hydrocarbon receptor nuclear translocator (ARNT) are expressed in developing mouse lung. *Am J Respir Crit Care Med* 2004;169:A662.
21. Levesque BM, Kong Y, Shan L, Sunday ME. PAS domain transcription factors (TFs) regulate early lung morphogenesis. *Am J Respir Crit Care Med* 2003;167:A381.
22. Goshu E, Jin H, Fasnacht R, Sepenski M, Michaud JL, Fan CM. Sim2 mutants have developmental defects not overlapping with those of Sim1 mutants. *Mol Cell Biol* 2002;22:4147–4157.
23. Springall DR, Collina G, Barer G, Suggett AJ, Bee D, Polak JM. Increased intracellular levels of calcitonin gene-related peptide-like immunoreactivity in pulmonary endocrine cells of hypoxic rats. *J Pathol* 1988;155:259–267.
24. Sonnenfeld MJ, Delvecchio C, Sun X. Analysis of the transcriptional activation domain of the Drosophila Tango bHLH-PAS transcription factor. *Dev Genes Evol* 2005;215:221–229.
25. Scherer LJ, Rossi JJ. Approaches for the sequence-specific knockdown of mRNA. *Nat Biotechnol* 2003;21:1457–1465.
26. Ten Have-Opbroek AAW. Lung development in the mouse embryo. *Exp Lung Res* 1991;17:111–130.
27. Sonis S, Haddad R, Posner M, Watkins B, Fey E, Morgan TV, Mookanamparambil L, Ramoni M. Gene expression changes in peripheral blood cells provide insight into the biological mechanisms associated with regimen-related toxicities in patients being treated for head and neck cancers. *Oral Oncol* 2007;43:289–300.
28. Li Y, Baker NE. Proneural enhancement by Notch overcomes Suppressor-of-Hairless repressor function in the developing Drosophila eye. *Curr Biol* 2001;11:330–338.
29. Austin CP, Feldman DE, Ida JA Jr, Cepko CL. Vertebrate retinal ganglion cells are selected from competent progenitors by the action of Notch. *Development* 1995;121:3637–3650.
30. Doi H, Iso T, Sato H, Yamazaki M, Matsui H, Tanaka T, Manabe I, Arai M, Nagai R, Kurabayashi M. Jagged1-selective notch signaling induces smooth muscle differentiation via RBP-Jkappa dependent pathway. *J Biol Chem* 2006;281:28555–28564.
31. Gao X, Chandra T, Gratton MO, Quelo I, Prud'homme J, Stifani S, St-Arnaud R. HES6 acts as a transcriptional repressor in myoblasts and can induce the myogenic differentiation program. *J Cell Biol* 2001; 154:1161–1171.
32. Lu J, Qian J, Izvolsky KI, Cardoso WV. Global analysis of genes differentially expressed in branching and non-branching regions of the mouse embryonic lung. *Dev Biol* 2004;273:418–435.
33. Billings PC, Herrick DJ, Howard PS, Kucich U, Engelsberg BN, Rosenbloom J. Expression of betaig-h3 by human bronchial smooth muscle cells: localization To the extracellular matrix and nucleus. *Am J Respir Cell Mol Biol* 2000;22:352–359.
34. Behr M, Riedel D, Schuh R, Fujita M, Itoh M, Shibata M, Taira S, Taira M. The claudin-like megatrachea is essential in septate junctions for the epithelial barrier function in Drosophila. *Dev Cell* 2003;5:611–620.
35. Haworth KE, El-Hanfy A, Prayag S, Healy C, Dietrich S, Sharpe P. Expression of Claudin-3 during chick development. *Gene Expr Patterns* 2005;6:40–44.
36. Sanford JL, Edwards JD, Mays TA, Gong B, Merriam AP, Rafael-Fortnoy JA. Claudin-5 localizes to the lateral membranes of cardiomyocytes and is altered in utrophin/dystrophin-deficient cardiomyopathic mice. *J Mol Cell Cardiol* 2005;38:323–332.
37. Wang DZ, Olson EN. Control of smooth muscle development by the myocardin family of transcriptional coactivators. *Curr Opin Genet Dev* 2004;14:558–566.
38. Pipes GC, Creemers EE, Olson EN. The myocardin family of transcriptional coactivators: versatile regulators of cell growth, migration, and myogenesis. *Genes Dev* 2006;20:1545–1556.
39. Brody JS, Vaccaro C. Postnatal formation of alveoli: interstitial events and physiologic consequences. *Fed Proc* 1979;38:215–223.